Characteristic features of symmetry breaking in two-component Bose-Einstein condensates

Jae Gil Kim and Eok Kyun Lee
Department of Chemistry and School of Molecular Science (BK 21), Korea Advanced Institute of Science and Technology, 373-1 Gusongdong, Yusongku, Taejon, Korea
(Received 19 September 2001; published 7 June 2002)

We examine the stability properties of the ground state of two-component Bose-Einstein condensates as a function of the interspecies interactions. A stability criterion is identified from the curvature matrix of the Gross-Pitaevskii energy functional subject to the normalization conditions. By analyzing the stability signature, the characteristic features of the spontaneous spatial symmetry breaking are verified in various types of traps. The details of the differences between the continuous symmetry breaking and discrete symmetry breaking are discussed.

DOI: 10.1103/PhysRevE.65.066201 PACS number(s): 05.45.−a, 02.70.−c, 03.75.Fi

I. INTRODUCTION

Recently two-component Bose-Einstein condensates (2BEC) have been realized by the systems of two different spin states of Rb in a magnetic trap [1,2] and, subsequently, Na in an optical trap [3]. Since then, a lot of theoretical works have focused on how the presence of the interspecies interactions affects the stability of the ground state structures and the excitation spectra of 2BEC. Different from the case of one-component BEC, 2BEC offers an opportunity to study a wide variety of interesting ground state structures such as phase separation and spontaneous spatial symmetry breaking due to an additional interspecies interaction. The phase separation of 2BEC has been first addressed in the Thomas-Fermi approximation [4] and studied more accurately within the Hartree-Fock theory [5,6]. In these studies, the ground state of 2BEC has been assumed to retain the spherical trap symmetry, so the phase separation proceeds with the forming of a central core dominated by one species with an outer shell of the second species. On the other hand, the symmetry-breaking phase separation of 2BEC, in which the ground state does not possess the symmetry of the trap potential, has been recently demonstrated numerically by solving the coupled Gross-Pitaevskii equations (GPEs) [7]. When the lowest excitation frequency becomes zero the symmetry-preserving ground state of 2BEC shows the onset of the instability and a subsequent transition to the symmetry-breaking state [8,9]. More recently, the effects of the trap geometry and finite temperature on the symmetry breaking were also investigated [10].

Until now most theoretical works on the spontaneous spatial symmetry breaking had used the approach based on the coupled Gross-Pitaevskii equations obtained from the optimum condition of the Gross-Pitaevskii energy functional (GPEF) [10,9]. However, it should be noted that the solutions of the GPEs do not always correspond to the local minimum of the GPEF since the set of solutions of the coupled GPEs also includes maxima and saddle points of the energy functional [8]. Therefore, it is more natural to investigate the stability properties of the ground state of 2BEC starting from the Gross-Pitaevskii energy functional. In this paper, we obtained the stationary solutions of the GPEF by applying the gradient projection method [11], which minimizes the GPEF subject to constant particle number. The specific symmetry-breaking states were obtained by imposing an additional symmetry constraints on the ground state wave function. After the determination of the stationary solutions of the GPEF, we investigated the stability properties of the stationary solutions by computing the eigenvalues of the curvature matrix of the GPEF subject to the normalization constraints. We found that, as crossing the instability point, the lowest eigenvalue of the curvature matrix, which corresponds to our stability criterion, becomes negative for the symmetry-preserving states making the excitation frequency purely imaginary, whereas it remains at zero or positive for the symmetry-breaking states depending on the broken symmetry. In earlier works, the stability of the ground state of 2BEC had been examined by computing the Hartree-Bogoliubov frequencies [8] or by solving the time-dependent GPEs under the modulation of the trap [12]. These stability analyses can only tell whether the stationary solutions are stable or not with respect to the time evolution. However, our stability criteria provide quantitative knowledge on the stability of the stationary solutions by identifying the saddleness of the stationary points on the GPEF surface.

The instabilities associated with the spontaneous spatial symmetry breaking can be classified according to the spatial symmetry of the resulting ground state. In general, the ground state of 2BEC breaks a symmetry in the direction corresponding to the weakest trap frequency [9]. However, the characteristic behaviors of the symmetry breaking show a marked difference depending on whether the broken symmetry is continuous or not. The invariance of the symmetry breaking under some continuous group produces a nonlocality in the critical solution set, which can be identified by the degeneracy of zero eigenvalue of the stability matrix [13]. These general behaviors accompanied with the instabilities in the symmetry breaking have not been studied in previous works. Our results show that the continuous symmetry breaking occurring in the radially symmetric trap or a pancakelike trap is always accompanied by the marginal stability, which implies the existence of an infinite number of degenerate symmetry-breaking states. The marginal stability can be noticed by occurrence of degenerate zero eigenvalues in the curvature matrix at the instability points. On the other hand, the discrete symmetry breaking in the cigarlike trap

proceeds by making the locally stable two degenerate states that are mirror images of each other.

In Sec. II, the basic theory and detailed numerical methods are explained. We define a different stability criterion from computation of the local curvatures of the Gross-Pitaevskii energy functional at the stationary points. In Sec. III, we present the numerical results of the symmetry breaking in various types of traps with a discussion of characteristic features of the continuous and discrete symmetry breaking. Finally, the conclusions and the limitation of our method are summarized in Sec. IV.

II. THEORY AND NUMERICAL COMPUTATION

We start by considering the Gross-Pitaevskii energy functional of 2BEC,

$$E[\Psi_1,\Psi_2]=\int d\mathbf{r}\Big(N_1\Psi_1^*\hat{h}_1\Psi_1+\lambda_m N_2\Psi_2^*\hat{h}_2\Psi_2 + \frac{g_{11}}{2}N_1^2|\Psi_1|^4+\lambda_m\frac{g_{22}}{2}N_2^2|\Psi_2|^4 + g_{12}N_1N_2|\Psi_1|^2|\Psi_2|^2\Big), \tag{1}$$

where N_j and Ψ_j are the number of atoms and the normalized wave function of jth condensate, respectively. Here, λ_m and λ_ω are the ratio of the mass and the radial frequency as m_1/m_2 and ω_1/ω_2, respectively. By scaling the length and energy with respect to the harmonic units of $l_1=\sqrt{\hbar/m_1\omega_1}$ and $\hbar\omega_1$, respectively, the one-body operators are given by $\hat{h}_j=-\nabla^2/2+(A_{jx}^2x^2+A_{jy}^2y^2+A_{jz}^2z^2)/2$, where $A_{2\alpha}=A_{1\alpha}/\lambda_m\lambda_\omega$ $(\alpha=x,y,z)$, $A_{j\alpha}$ being the anisotropic parameter along the axis α for the species j. We approximate the atomic interactions as the pseudopotential $g_{ij}=2\pi\hbar^2a_{ij}/m_{ij}$, where m_{ij} is the reduced mass defined by $1/m_{ij}=1/m_i+1/m_j$, and a_{ij} is the s-wave scattering length between the species i and j. By same scaling, $g_{11}=4\pi a_{11}/l_1$, $g_{22}=4\pi a_{22}/l_1$, and $g_{12}=(1+\lambda_m)2\pi a_{12}/l_1$.

At zero temperature the condensate wave functions of jth component Ψ_j obeys the time-dependent Gross-Pitaevskii equations $i\partial\Psi_j/\partial t=\delta E/\delta\Psi_j^*$. Various numerical techniques have been applied to determine the stationary solutions of time-dependent GPEs [15–17]. Here we take a different approach by transforming the Hamiltonian systems to the gradient systems whose dynamics is governed by the diffusion equations $\partial\Psi_j/\partial\tau=-\delta E/\delta\Psi_j^*=f[\Psi_j]$, where τ is the imaginary time it. Then $f[\Psi_j]$ can be considered as a force that is derived from the negative gradient of the potential function $E[\Psi_1,\Psi_2]$ with respect to Ψ_j^*. Thus the minimizing process of E is equivalent to a process of finding stationary states of $\Psi_j(\tau)$ and the stability properties of the stationary states are determined from the local curvatures of the GPEF subject to the normalization constraints. The condensate wave function Ψ_j are assumed to be real, since any phase factor can be trivially eliminated. By expanding Ψ_j with the harmonic oscillator basis as $\Psi_j=\Sigma c_\alpha^j\phi_\alpha^j$, the GPEF reduces to a finite dimensional form as

$$E[c_\alpha^1,c_\beta^2]=N_1\sum\ \epsilon_\alpha^1|c_\alpha^1|^2+\lambda_m N_2\sum\ \epsilon_\alpha^2|c_\alpha^2|^2 + \frac{g_{11}}{2}N_1^2\sum\ c_\alpha^1c_\beta^1c_\gamma^1c_\delta^1Z_{\alpha\beta\gamma\delta}^{1111} + \lambda_m\frac{g_{22}}{2}N_2^2\sum\ c_\alpha^2c_\beta^2c_\gamma^2c_\delta^2Z_{\alpha\beta\gamma\delta}^{2222} + g_{12}N_1N_2\sum\ c_\alpha^1c_\beta^1c_\gamma^2c_\delta^2Z_{\alpha\beta\gamma\delta}^{1122}, \tag{2}$$

where $\hat{h}_j\phi_\alpha=\epsilon_\alpha^j\phi_\alpha$ and $Z_{\alpha\beta\gamma\delta}^{ijkl}=\int d\mathbf{r}\phi_\alpha^i\phi_\beta^j\phi_\gamma^k\phi_\delta^l$. The stationary states of Eq. (1) corresponding to optima of the GPEF are obtained by minimizing Eq. (2) subject to the constraints of constant particle numbers, i.e., by the condition $G_j(c_\alpha^j)=\Sigma|c_\alpha^j|^2-1=0$. We used the gradient projection technique that minimizes E iteratively along the gradient projected onto the linear subspace defined by the constraint set [11]. The projection matrix $\mathbf{P}$ is defined as $\mathbf{I}-\mathbf{u}_1\otimes\mathbf{u}_1-\mathbf{u}_2\otimes\mathbf{u}_2$, where $\mathbf{I}$ is $2N_{basis}\times2N_{basis}$ identity matrix, and $\mathbf{u}_1$ and $\mathbf{u}_2$ are normalized $2N_{basis}$ dimensional column vectors spanning the linear constraints subspace identical to $(c_\alpha^1,\mathbf{0})^T$ and $(\mathbf{0},c_\beta^2)^T$, respectively. Here $\otimes$ means the ''outer'' product of two vectors. The gradient projection method forces Ψ_j to converge to the lowest energy state. To find a specific symmetry-breaking state, we have to impose an additional symmetry constraint on Ψ_j.

The stability of stationary states can be identified by examining the eigenvalues of the curvature matrix of the Gross-Pitaevskii energy functional. The curvature matrix is obtained by projecting the Hessian matrix of the GPEF on the subspace defined by the constraint set, i.e., $\mathbf{H}^{proj}=\mathbf{P}^T\mathbf{H}\mathbf{P}$, $\mathbf{H}=\partial^2E/\partial c_\alpha^i\partial c_\beta^j$. Notice that the normalization constraints G_j restrict the fluctuations of c_α^j around the stationary points. The normal modes of $\mathbf{H}^{proj}$ are decomposed into two subspaces. One subspace corresponds to the constraint space composed of $\mathbf{u}_1$ and $\mathbf{u}_2$, and the other subspace corresponds to the orthogonal subspace whose normal modes are orthogonal to both $\mathbf{u}_1$ and $\mathbf{u}_2$. The onset of the instability and the transition to the symmetry-breaking states occur when the lowest eigenvalue of $\mathbf{H}^{proj}$ in the orthogonal subspace becomes zero. At the instability point, the direction of the symmetry-breaking solution is determined uniquely by the eigenvector with zero eigenvalue. Our stability criterion also provides the degree of the stability of the stationary solutions by identifying a saddleness of the stationary point on the GPEF surface. Indeed, we found that the symmetry-preserving and symmetry-breaking states correspond to 1 saddle and 0 saddle, respectively, in the symmetry-breaking parameter regime. Here, i saddle means a saddle point of the GPEF surface, which has i negative eigenvalues. The number of degeneracy of eigenvalues, which become zero at the instability point depends on the symmetry of the trap. It is threefold degenerate for a radially symmetric trap, and twofold degenerate for a pancakelike trap. Finally, for a cigarlike trap, it is nondegenerate.

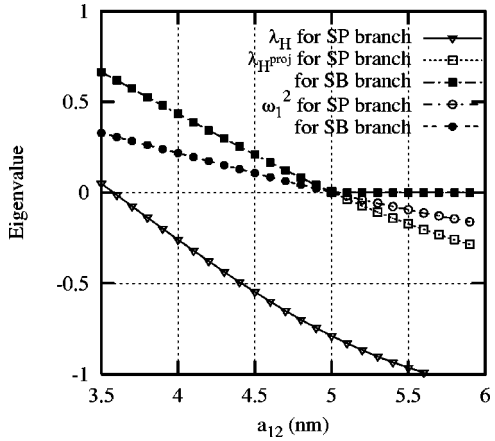

FIG. 1. The values of $\lambda_{\mathbf{H}^{proj}}$, $\lambda_{\mathbf{H}}$, and ω_1^2 vs interspecies coupling constant a_{12} in a radially symmetric trap. Symmetry-preserving branch and symmetry-breaking branch are abbreviated by SP and SB, respectively.

III. RESULTS AND DISCUSSIONS

We first carried out calculations with the same parameter set as used in the work of Pu and Bigelow [14] for comparison. We assumed Rb as component 1 and Na as component 2 with intraspecies scattering lengths of 6 nm and 3 nm, respectively. The radial trap frequencies were taken as $\omega_1 = 2\pi \times 160$ Hz and $\omega_2 = 2\pi \times 310$ Hz. In Fig. 1 the lowest eigenvalue of $\mathbf{H}^{proj}$ ($\lambda_{\mathbf{H}^{proj}}$) and $\mathbf{H}$ ($\lambda_{\mathbf{H}}$) for the case of a radially symmetric trap were plotted for the symmetry-preserving and symmetry-breaking solutions, respectively, as a function of the interspecies scattering length a_{12} for fixed $N_1 = N_2 = 10^3$. The closed and open squares represent $\lambda_{\mathbf{H}^{proj}}$ corresponding to the symmetry-breaking states and symmetry-preserving states, respectively. Notice that, as a_{12} crosses the instability point ($a_{12} = 5.0$), $\lambda_{\mathbf{H}^{proj}}$ becomes negative for the symmetry-preserving states, whereas it remains at zero for the symmetry-breaking states. This shows that the occurrence of the instability of the symmetry-preserving state is always accompanied with the symmetry-breaking state that is marginally stable. If the symmetry breaking is invariant under some continuous group, the critical solution sets are nonlocal in nature with one or two more eigenvalues of the stability matrix being zero. In the radially symmetric trap, L^2 rotational symmetry becomes broken and the resulting symmetry-breaking states are degenerate under the L^2 symmetry operation. Thus lowest eigenvalues of $\mathbf{H}^{proj}$ for the symmetry-preserving branch are threefold degenerate and become zero simultaneously at the instability point. As expected, $\lambda_{\mathbf{H}}$ for the symmetry-preserving solution, denoted by the open triangles, becomes negative prior to the onset of the instability (see Fig. 1). Indeed, the semipositive definiteness of $\mathbf{H}$ is only sufficient condition for the stable solution since it accounts for the stability with respect to arbitrary nonzero fluctuations including number of particles. To confirm this, the square of the Hartree-Bogoliubov frequency ω_1^2 for the symmetry-preserving solutions is plotted with open circles in Fig. 1. In the symmetry-breaking parameter regime, ω_1 becomes purely imaginary. It implies that the fluctuations of the condensates grow exponentially with time. On the other hand, for the symmetry-breaking solutions, ω_1 becomes zero at the critical value a_{12}^c and stays at zero even for $a_{12} > a_{12}^c$, implying the marginal stability of the symmetry-breaking state. It is consistent with the fact that $\lambda_{\mathbf{H}^{proj}}$ remains at zero for $a_{12} > a_{12}^c$. The point where ω_1 becomes complex exactly coincides with the instability point defined by our criterion $\lambda_{\mathbf{H}^{proj}} = 0$.

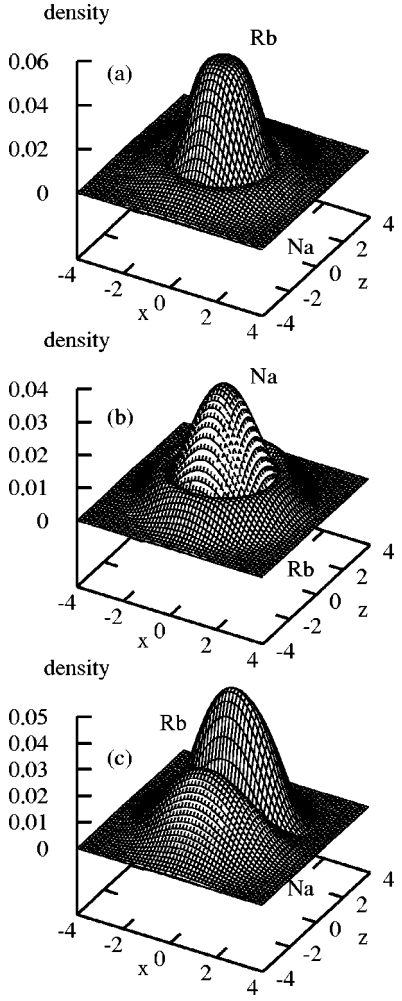

FIG. 2. The spatial density profiles of the phase separated, but symmetry-preserving state at $z = 0$ plane Rb core with surrounding Na atoms (a), Na core with surrounding Rb atoms (b). The spatial density profile of the symmetry-breaking state (c). Here, $a_{12} = 9.6$ nm and the spatial coordinates are scaled by the harmonic oscillator length l_1.

Our study also revealed that two types of phase separated, but symmetry-preserving solutions at $a_{12} = 9.6$ nm, which had been believed to be a ground state [Rb core with surrounding Na atoms in Fig. 2(a)] and a metastable state [Na core with surrounding Rb atoms in Fig. 2(b)], actually correspond to saddle points of the energy functional E. The $\lambda_{\mathbf{H}^{proj}}$ for Figs. 2(a) and 2(b) states shows negative values, -0.702 and -1.557, respectively. Therefore, in this parameter regime, the only stable state is the symmetry-breaking state [see Fig. 2(c)]. The energies for Figs. 2(a), 2(b), and 2(c) states are realized as $E_{2(a)}/N_1 = 9.556$, $E_{2(b)}/N_1 = 10.009$, and $E_{2(c)}/N_1 = 9.269$, respectively. However, if

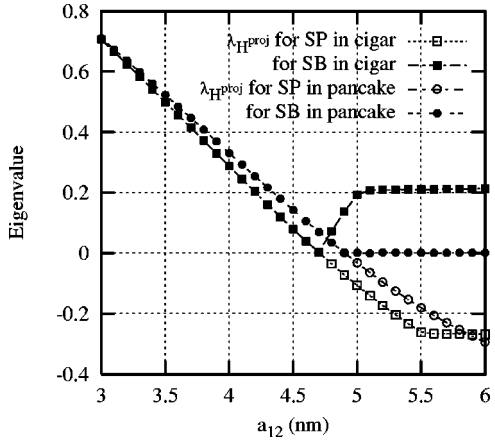

FIG. 3. The value of $\lambda_{\mathbf{H}^{proj}}$ for the symmetry-preserving and symmetry-breaking branches as a function of a_{12} in a cigarlike and pancakelike trap.

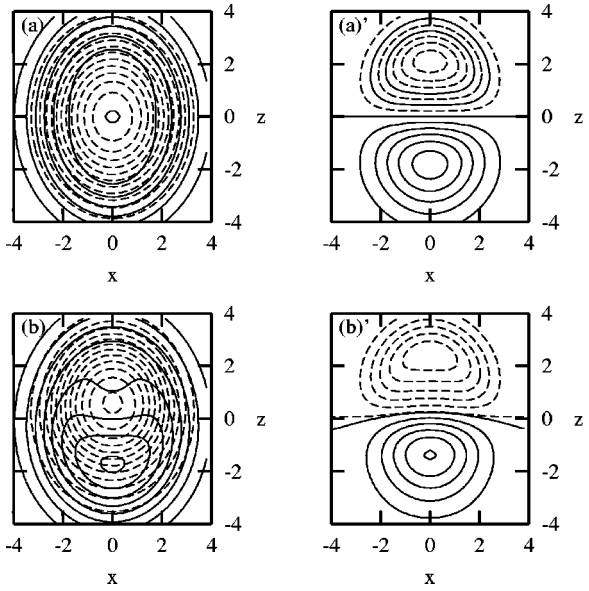

FIG. 4. The contour density profiles of the condensates and eigenvectors $\delta\psi_j(j=1,2)$ in a cigarlike trap in $z=0$ plane for $a_{12}=4.7$. (a) Phase separated, but symmetry-preserving state, (b) symmetry-breaking state along the z axis obtained by adding (a′) to (a). (a′) and (b′) are eigenvectors corresponding to (a) and (b), respectively. Here, the spatial coordinates are scaled by the harmonic oscillator length l_1.

we impose the constraint that requires the solutions to be symmetry preserving, the states in Figs. 2(a) and 2(b) become local minima in the constrained subspace of energy functional E due to the symmetry-preserving constraint. In the constrained subspace, Fig. 2(b) state can be considered as the metastable one that relaxes slowly to the Fig. 2(a) state by applying the symmetry-preserving perturbations. The transition from Fig. 2(b) to Fig. 2(a) was pointed out by the nonlinear response analysis under radially symmetric off-resonance modulations of the trapping potential [14].

When the system is in the symmetry-breaking parameter regime, the ground state of 2BEC breaks a symmetry in the direction corresponding to the weakest trap frequency. Therefore, in a cigarlike cylindrically symmetric trap, the discrete z-parity symmetry Π_z is broken and two degenerate symmetry-breaking states that are mirror images of each other with respect to the xy plane appear. On the other hand, in a radially symmetric trap, the continuous rotational symmetry L^2 is broken and an infinite number of degenerate symmetry-breaking states, whose orientation of the symmetry axis is random, appear. However, in the symmetry-breaking parameter regime, the characteristic feature of $\lambda_{\mathbf{H}^{proj}}$ shows a marked difference depending on whether the symmetry breaking is continuous or not. For the case of continuous symmetry breaking, $\lambda_{\mathbf{H}^{proj}}$ remains at zero, showing that it is neither in a stable state nor in an unstable state. It implies that the symmetry-breaking state has an infinite number of degeneracy due to the invariance of symmetry breaking with respect to a broken symmetry. In contrast, for the case of discrete symmetry breaking, $\lambda_{\mathbf{H}^{proj}}$ becomes positive again in the symmetry-breaking parameter regime. In Figs. 3(a) and 3(b), we plotted $\lambda_{\mathbf{H}^{proj}}$ for both cases of the symmetry-preserving and symmetry-breaking solutions in the pancakelike trap ($A_{1x}=A_{1y}=0.8$ and $A_{1z}=1.0$) and cigarlike trap ($A_{1x}=A_{1y}=1.0$ and $A_{1z}=0.8$), respectively. The characteristic feature of $\lambda_{\mathbf{H}^{proj}}$ for the case of a pancakelike trap is the same as that for a radially symmetric trap except that the number of degeneracy of $\lambda_{\mathbf{H}^{proj}}$ is two (see Fig. 1). In a pancakelike trap, the marginal stability is due to the existence of an infinite number of degenerate symmetry-breaking states retaining a plane of symmetry that include the z axis, but whose orientation is random. On the other hand, the discrete z-parity symmetry-breaking states in the cigarlike trap correspond to local minimums of the energy functional E since $\lambda_{\mathbf{H}^{proj}}>0$.

At the instability points, the eigenvector $\mathbf{e}_{\lambda_{\mathbf{H}^{proj}=0}}$ of zero eigenvalue $\lambda_{\mathbf{H}^{proj}}=0$ determines the initial direction of a new bifurcating solution. In Figs. 4(a) and 4(a′), we plot the symmetry-preserving states of each component and their eigenvectors in a cigarlike trap at the critical value $a_{12}^c=4.7$. The symmetry-preserving state in Fig. 4(a) is a phase separated one where Na atoms surround Rb core atoms. The solid and dashed lines correspond to the condensate profile of Rb and Na, respectively. The density profiles of the eigenvectors for each component are composed of $\delta\psi_j=\Sigma_\alpha(\mathbf{e}_{\lambda_{\mathbf{H}^{proj}=0}})_\alpha\phi_\alpha^j$ $(j=1,2)$, respectively. Since $\lambda_{\mathbf{H}^{proj}}$ is nondegenerate in the cigarlike trap, the density profiles of $\mathbf{e}_{\lambda_{\mathbf{H}^{proj}=0}}$ in Fig. 4(a′) determine a unique direction of newly bifurcating solution, which has symmetry breaking along the z axis. We confirmed that the direction of the symmetry breaking at $a_{12}=4.8$ as shown in Fig. 4(b) coincide with the polarization direction of $\mathbf{e}_{\lambda_{\mathbf{H}^{proj}=0}}$. The direction of the eigenvector of Fig. 4(b) also coincides with the direction of the symmetry-breaking solution along the z axis as can be seen in Fig. 4(b′). The other degenerate state of the symmetry-breaking solution, which is mirror image of Fig. 4(b), can be obtained by adding the eigenvector of zero eigenvalue in the opposite direction to Fig. 4(a) as $-\mathbf{e}_{\lambda_{\mathbf{H}^{proj}=0}}$.

Furthermore, $\mathbf{e}_{\lambda_{\mathbf{H}^{proj}=0}}$ also plays an important role in constructing new degenerate symmetry-breaking states for the

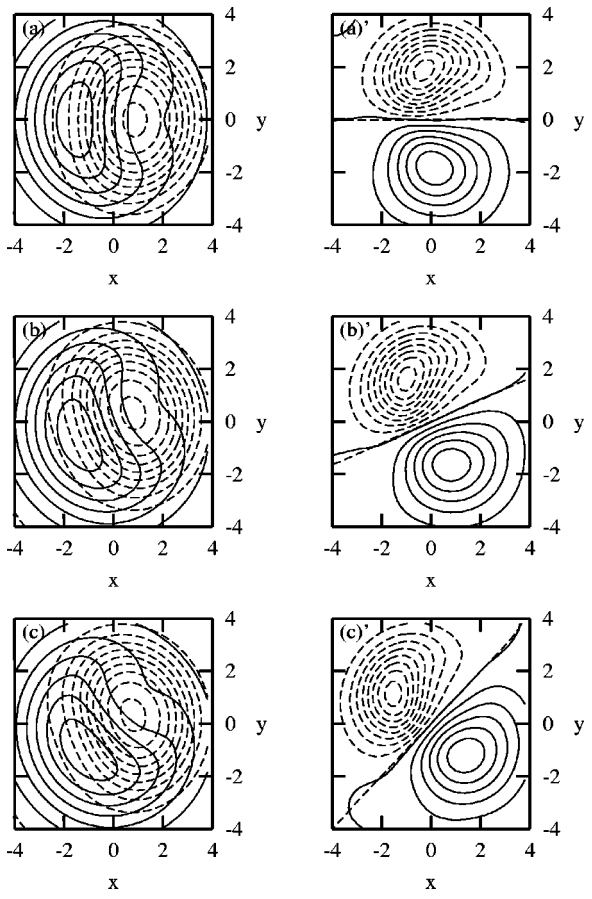

FIG. 5. The contour density profiles of the condensates and eigenvector directions $\delta\psi_j^0(j=1,2)$ in a pancakelike trap in $z=0$ plane for $a_{12}=5.3$. (a) Symmetry-breaking state along the x axis, (b) slightly counterclockwise-rotated symmetry-breaking state obtained by adding (a′) to (a), (c) further rotated symmetry-breaking state obtained by adding (b′) to (b). (a′), (b′), and (c′) are eigenvectors corresponding to (a), (b), and (c), respectively. Here, the spatial coordinates are scaled by the harmonic oscillator length l_1.

case of the continuous symmetry breaking where the stability is marginal ($\lambda_{\mathbf{H}^{proj}}=0$). In Fig. 5 we plot the condensate wave functions and corresponding eigenvectors profiles $\delta\psi_j$ in the pancakelike trap at the symmetry-breaking parameter regime $a_{12}=5.2$. The initial state in Fig. 5(a) is a symmetry-breaking state along the x axis. It produces the eigenvectors of $\lambda_{\mathbf{H}^{proj}}=0$ whose profiles are polarized along the y axis as shown in Fig. 5(a′). The addition of Fig. 5(a′) to Fig. 5(a) and the subsequent optimization gives the slightly counterclockwise-rotated symmetry-breaking state in Fig. 5(b). The eigenvectors of $\lambda_{\mathbf{H}^{proj}}=0$ corresponding to the state in Fig. 5(b) become the one in Fig. 5(b′),which is counterclockwise-rotated one as compared to that in Fig. 5 (a′). Next, addition of Fig. 5(b′) to Fig. 5(b) produces the further counterclockwise-rotated symmetry-breaking state of Fig. 5(c).

IV. SUMMARY

We investigated the stability properties of the ground state of 2BEC as a function of the interspecies interactions within the framework of the Gross-Pitaevskii energy functional. The stability criterion indicated by the sign of $\lambda_{\mathbf{H}^{proj}}$ provides a necessary and sufficient condition for the onset of the instability associated with the spontaneous spatial symmetry breaking in the ground states of 2BEC. Also the characteristic features of the spontaneous spatial symmetry breaking for both continuous and discrete cases were investigated by examining the stability signature in the symmetry-breaking parameter regime.

In the present study, our main concern is about the stability problems of the ground states of 2BEC associated with the symmetry breaking. Recently, there have been several theoretical efforts to understand the phase separation of 2BEC in the presence of vorticity [18]. Our stability analysis can be extended to a more complicated case of the phase separation of 2BEC associated with a creation of quantized vortex or soliton. However, to investigate the stability and dynamics of 2BEC creating a vortex or soliton, the phase contributions of the condensate wave function have to be explicitely considered in the Gross-Pitaevskii energy functional. Here we used the fact that the ground state of 2BEC can be expressed by a real wave function with a constant phase. So, our stability analysis is actually restricted to the real stationary solutions of the Gross-Pitaevskii energy functional.

ACKNOWLEDGMENTS

We acknowledge that this work was supported in part by KOSEF (Grant No. NL06990), and in part by BK21, School of Molecular Science.

[1] C.J. Myatt, E.A. Burt, R.W. Ghrist, E.A. Cornell, and C.E. Wieman, Phys. Rev. Lett. **78**, 586 (1997).
[2] D.S. Hall, M.R. Matthews, J.R. Ensher, C.E. Wieman, and E.A. Cornell, Phys. Rev. Lett. **81**, 1539 (1998).
[3] D.M. Stamper-Kurn, M.R. Andrews, A.P. Chikkatur, S. Inouye, H.J. Miesner, J. Stenger, and W. Ketterle, Phys. Rev. Lett. **80**, 2027 (1998).
[4] T.L. Ho and V.B. Shenoy, Phys. Rev. Lett. **77**, 3276 (1996).
[5] B.D. Esry, C.H. Greene, J.P. Burke, and L. Bohn, Phys. Rev. Lett. **78**, 3594 (1997).
[6] H. Pu and N.P. Bigelow, Phys. Rev. Lett. **80**, 1130 (1998).
[7] P. Ohberg and S. Stenholm, Phys. Rev. A **57**, 1272 (1998).
[8] D. Gordon and C.M. Savage, Phys. Rev. A **58**, 1440 (1998).
[9] B.D. Esry, Phys. Rev. A **58**, R3399 (1998); B.D. Esry and C.H. Greene, *ibid.* **59**, 1457 (1999).
[10] P. Ohberg, Phys. Rev. A **59**, 634 (1999); **61**, 013601 (2000).
[11] D. A. Wismer and R. Chattergy, *Introduction to Nonlinear Optimization* (Elsevier/North-Holland, New York/Amsterdam, 1978).
[12] C.K. Law, H. Pu, N.P. Bigelow, and J.H. Eberly, Phys. Rev.

Lett. **79**, 3105 (1997).
[13] R. Gilmore, *Catastrophy Theory for Scientists and Engineers* (Wiley, New York, 1981).
[14] H. Pu and N.P. Bigelow, Phys. Rev. Lett. **80**, 1134 (1998).
[15] F. Dalfovo and S. Stringari, Phys. Rev. A **53**, 2477 (1996).
[16] M. Edwards, R.J. Dodd, C.W. Clark, P.A. Ruprecht, and K. Burnett, Phys. Rev. A **53**, R1950 (1966).
[17] J.G. Kim, K.K. Kang, B.S. Kim, and E.K. Lee, J. Phys. B **33**, 2559 (2000).
[18] S.T. Chui, V.N. Ryzhov, and E.E. Tareyeva, Phys. Rev. A **63**, 023605 (2001); D.M. Jezek, P. Capuzzi, and H.M. Cataldo, *ibid.* **64**, 023605 (2001).